Transactions, SMiRT-24
BEXCO, Busan, Korea - August 20-25, 2017
Division II - Fracture Mechanics and Structural Integrity

3D DYNAMIC FRACTURE AND FRAGMENTATION OF AGR GRAPHITE BRICK SLICES USING XCZM

T. Crump[1], S. Mundy[2], A. Jivkov[3], P. Mummery[4], G Ferté[5], V.X Tran[6]

[1] EngD Student, MACE, University of Manchester, UK
[2] Undergraduate Student, MACE, University of Manchester, UK
[3] Senior Lecturer, MACE, University of Manchester, UK
[4] Professor, MACE, University of Manchester, UK
[5] Research Engineer, EDF R&D AMA, France
[6] Manager, EDF Energy R&D UK Centre, UK

ABSTRACT

It has been anticipated and recently observed that axial cracks can occur at keyway corners of graphite bricks in the UK Advanced Gas-cooled Reactors (AGR). The crack initiation is triggered by internal stress reversal during reactor operation and may potentially lead to brick more cracks through a mechanism known as Prompt Secondary Cracking (PSC). To assess the likelihood of this occurring, a method for modelling dynamic fracture, known as eXtended Finite Element Method with cohesive elements (XCZM), is used to analyse whole 3D component fragmentation. Within this work, XCZM is used to model primary crack interactions with a methane hole and secondary crack profiles in a 3D brick slice under external hoop stress loading.

KEYWORDS: Elastodynamics, Graphite, Prompt Secondary Cracking, Quasi-explicit, XCZM

INTRODUCTION

The main reactor type in the UK is the Advanced Gas-cooled Reactor (AGR). The 14 AGR's currently in operation are coming up to the autumn years of their initial projected life span. Considering the UK's commitment to low-carbon generation there is scope for Plant-Life Extension (PLEX) while the next generation of reactors are being commissioned, ONR, DECC (2015). One of the challenges, highlighted as a life-limiting factor of the AGR's, is cracking of the graphite core, first observed in 2014 (Figure 1(a)). This is because the 6000+ graphite bricks in an AGR, see Figure 1(b), provide not only the main neutron moderation of the fission reaction but also some of the structural integrity support for the core. Consequently, graphite brick integrity is significantly more important within AGR's compared to other graphite reactor types, such as the High Power Channel-type Reactor (RBMK's).

One of the postulated consequences of the initial 'Primary' keyway cracking, which occurs post stress turnaround, see Figure 2(a), is Prompt Secondary Cracking (PSC). The PSC mechanism is considered to be driven by the superposition of shear strain waves generated by the opening of the first axial crack, which could initiate a second axial crack in one or more of the other keyway corners as shown schematically in Figure 2(b).

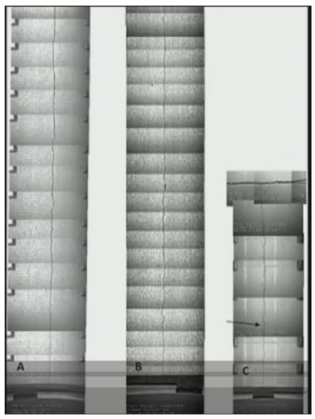

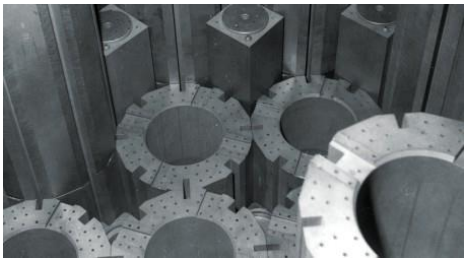

(a) (b)

Figure 1. (a) Keyway root crack observed at Hunterston B; (b) AGR core which contains 6000+ graphite bricks, BBC News (2016), IAEA (2016), Neighbour (2007).

To investigate this mechanism, a method for modelling dynamic fracture, known as the eXtended Finite Element Method with cohesive elements (XCZM), has been developed in Code_Aster and used here to study macro-scale fragmentation in 3D.

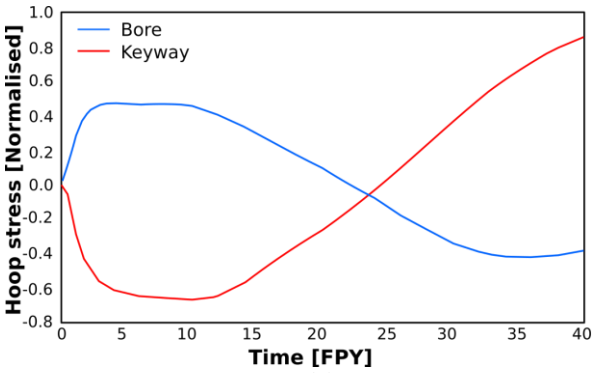

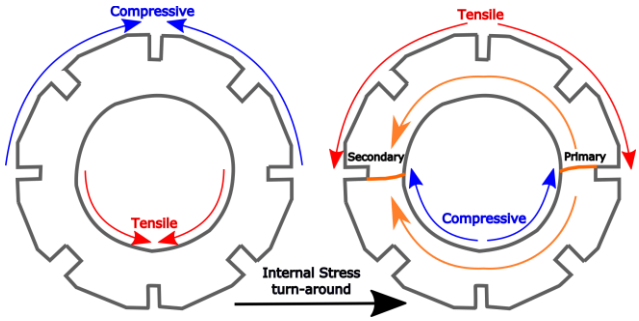

(a) (b)

Figure 2. (a) Normalised through-life stresses in a typical AGR graphite moderator brick. The change stress every 2 Full Power Years (FPY) is caused by thermal stress at shut-down, Marsden (2016); (b) Schematic of the Prompt Secondary Cracking mechanism.

This paper extends and builds upon previous works in 2D and 3D brick slices under hoop-stress loading using XCZM, Crump (2016, 2017). Here, a recently developed multi-crack algorithm is used to allow n-number of independent on-the-fly cracks to be incorporated into a single model to investigate and observe:

- interaction of an on-the-fly crack with a methane hole;
- periodic potential effects a on cracks profile;
- secondary crack profile.

DYNAMIC FRACTURE

Most industrial investigations of fracture are limited to quasi-static propagation due to computational power constraints. Consequently, some of the physical processes, which occur due to dynamic loading of a material, are neglected. However, fracture is a dynamic process and is often only considered when material inertia becomes significant. This is to say that with dynamically-loaded cracks, inertia, rate-dependent material behaviour and reflected strain waves become more important with the solid body

subjected to a time-dependent load, Freund (1990). Dynamic loads give rise to high stress levels near the crack-tip, leading to rapid crack propagation, which does not allow sufficient time for plastic deformations to develop. Therefore, energy is released within a short time frame from a crack in the form of kinetic energy, in 3D via Dilation waves, Shear/Rayleigh waves and Flexural waves (Figure 3(a)), rather than as an instantaneous change in Potential Energy as with quasi-static fracture, Meyers (1994). Each of the waves has a different energy dissipation rate leading to a complex combined strain wave (Figure 3(b)). This strain wave propagates affecting the stress state of the material remotely to the dynamic fracture event as seen in Figure. 3(c), Meyers (1994).

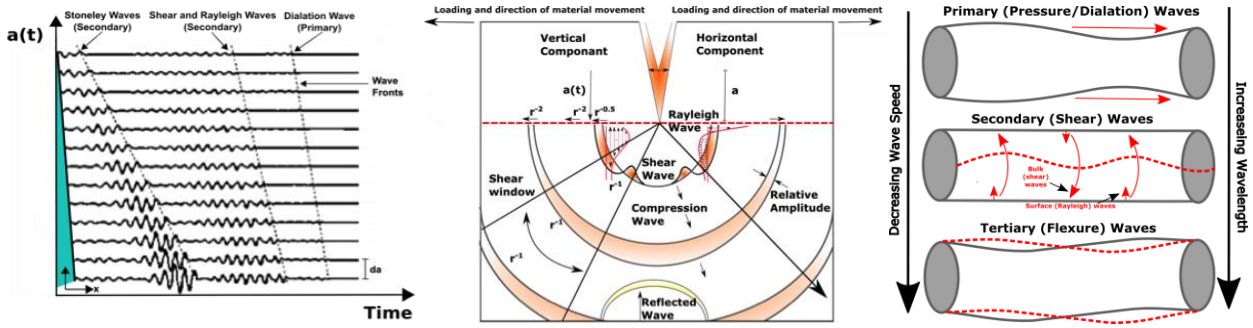

(a) (b) (c)

Figure 3. (a) Waves produced by a propagating crack; (b) combined propagating strain wave due to a propagated crack; (c) loading effects in 3D of a cylinder under loadings.

The elastodynamic strain energy release rate for a steady state propagating crack is:

$$G(t) = \frac{1}{2}\frac{d}{da}\left[\frac{\pi\sigma^2 a}{E} - \frac{k}{2}\rho a^2\dot{a}^2\left(\frac{\sigma}{E}\right)\right] = 2\gamma, \tag{1}$$

where a is the crack length, ρ the material density, E the elastic modulus, σ is the remotely applied stress, k is a constant dependant on crack speed (wavenumber) and γ is the material free surface energy, Freund (1990). Equation (1) specifies whether a crack will extend or remain stationary through a fracture criterion such as when $G(t)>G_c$ or in terms of the Mode I fracture toughness, $K(t)>K_{Ic}$. The fracture toughness is considered to be a material property derived through static fracture toughness testing. However, due to the increased kinetic energy, dynamic fracture can occur below these critical limits and thus K_I can be seen as a function of the crack velocity with the limiting velocity being that of the speed of sound within a material, known as the Rayleigh Wave speed, c_r. The relationship between crack velocity and the static fracture toughness can be written as

$$\dot{a} = c_r\left(1 - \frac{K_{IC}}{K_I^d}\right), \tag{2}$$

where K_I^d is the dynamic stress intensity, Kanninen and Popelar (1985). Through extensive experiments it has been observed that dynamic cracks do not exceed $0.7c_r$ in reality due to geometrical effects and the limits of linear elastic assumptions of a homogenous isotropic material, not taking into account the micro-textural influence on the propagating crack, K. Ravi-Chandar and W.G. Knauss (1984). These assumptions are however valid to a significant degree for AGR graphite, which is seen to become increasingly more brittle as a result of irradiation, Bradford (2008). Unstable dynamic fracture also produces straighter/closer to planar cracks because of a smaller fracture process zone, due to the material having less time to produce yielding or a damage zone. This leads to a sharper crack front with micro-cracks rather than voids ahead of the propagating crack, Meyers (1994).

Another feature of dynamic fracture, which can be considered as a multi-scale effect, is the velocity toughening felt by a crack-tip as it accelerates within a material. Velocity toughening results from

different features produced at different velocities, yielding different fracture toughness values, as illustrated in Figure 4. Toughening can be described by a simple empirical expression, Zhou (2005):

$$G_c(\dot{a}_0) = G_0 \log\left(\frac{\dot{a}_L}{\dot{a}_L - \dot{a}_0}\right) \tag{3}$$

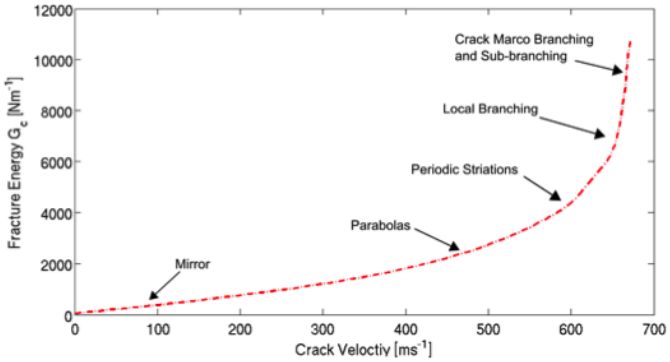

Figure 4. Velocity toughening curve and features observed, Zhou (2005).

MODELLING APPROACH

The optimal approach for any model is one that is 'mesh independent' while representing the required physics as accurately as possible. The XCZM approach aims to do this through combining the eXtended Finite Element Method (XFEM) and cohesive zone modelling (CZM). XFEM is used to represent the crack lips, Figure 5(a), by inserting Heaviside step functions into the standard element shape functions

$$u(x) = \sum_i a_i\, N_i(x) + \sum_i b_i\, N_i(x)\, H(x), \tag{4}$$

where N(x) is the classical function and H(x) is the Heaviside step function, while CZM is used to represent the failure criterion through a cohesive law.

Crack tip representation

The crack tip behaviour is represented through a cohesive zone law, which takes the meso-scale velocity toughening in Equation 3 into account (See Figure 5(b)):

$$\delta_c(\dot{a}) = \delta_0 \log\left(\frac{\dot{a}_L}{\dot{a}_L - \dot{a}_0}\right) \tag{5}$$

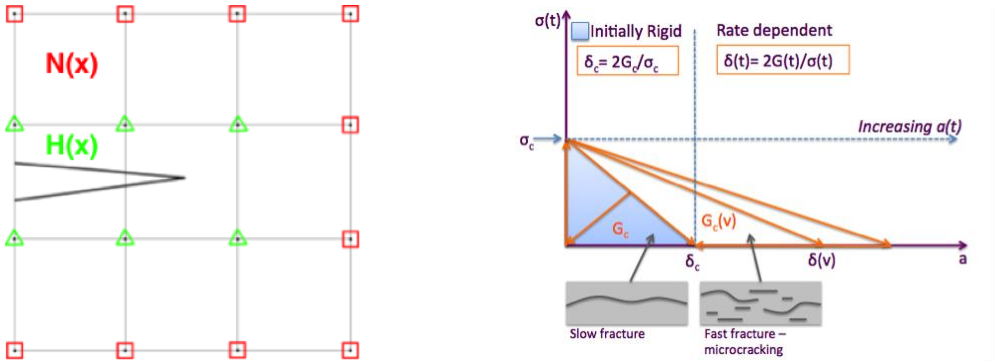

(a) (b)

Figure 5. (a) XFEM crack representation: triangles are enriched with discontinuous Heaviside function and squares are the classical Finite element function; (b) Intially rigid opening rate-dependant cohesive law, Doyen (2013), Moës (1999), Zhou (2005).

Cohesive zone models also come with a characteristic length, which at zero velocity is:

$$l_c(\dot{a}=0) = M\left(\frac{G_C E}{{\sigma_c}^2(1-\nu^2)}\right) \tag{6}$$

The cohesive zone is then integrated into the model through a quasi-explicit solver with the energy flux intergral in Figure 6(a) being, Crump (2017), Doyen (2013):

$$F(\Gamma_{coh}) = F\left(\Gamma_{appl}\right) \tag{7}$$

where the G, K, Crack Opening Displacement (COD) are related via, Freund (1990):

$$G_{ext} = -G_c = \frac{1-\nu^2}{E}\left({K_I}^2 + {K_{II}}^2\right) + \frac{1}{2\mu}{K_{III}}^2 = \sigma_c \delta \tag{8}$$

and the 3D crack bifurcation angle determined through the Rankine Criterion (see Figure 6(b)):

$$\beta = \frac{1}{2}\tan^{-1}\left(\frac{2\sigma_{nt}}{\sigma_{nn}-\sigma_{tt}}\right) \tag{9}$$

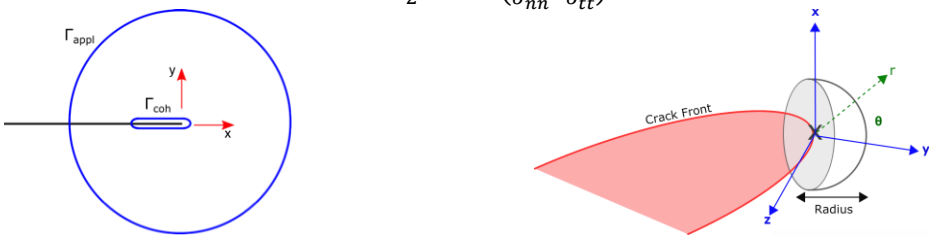

(a) (b)

Figure 6. (a) Intergration of the choesive zone into a model; (b) Deterimination of the bifurcation angle, Ferté (2014), Freund (1990).

The model has been demonstrated to provide converging solutions through the use of a quasi-explicit solver when the CFL criterion is met such that, Crump (2017):

$$\Delta t_c^{XFEM} = \frac{\Delta t_c^{XFEM}}{2} = \frac{h_{\min}}{c_d} \tag{10}$$

Multiple crack algorithum

To be able to model muliple on-the-fly XCZM cracks which are able to independently initiate, propagate and arrest, an algorithm has been developed as can be seen in Figure 7. The algorithm comes in the form of a supervisory macro which allows the crack to be governed by the cohesive law and managed based on test questions at each call of the XCZM algorithm. At each test the crack is then put into an array list at each time step:

- P_FISS - calculate angle and allow to propagate,
- PN_FISS - do not calculate angle and allow to propagate,
- N_FISS - has not initiated,
- A_FISS - arrested crack,
- AA_FISS - cracks that have fully arrested by breaking through a boundary.

The reasoning behind PN_FISS is that the angle calculation needs to be done as close to the cohesive characteristic length as possible to find a convergent crack path without user intervention. If the algorithm

is called at a small enough time-step to ensure that this is the case, then a crack that has propagated far enough to have the angle calculated will be moved from PN_FISS to P_FISS. This propagation length is governed by a parameter, da_max, which must always be long enough to allow for the full crack propagation within that time-step. This parameter is then used to consider if a crack is close to a boundary by calculating the relative distance. If the relative distance is smaller than da_max then the crack is forced to propagate straight to break through the geometric boundary.

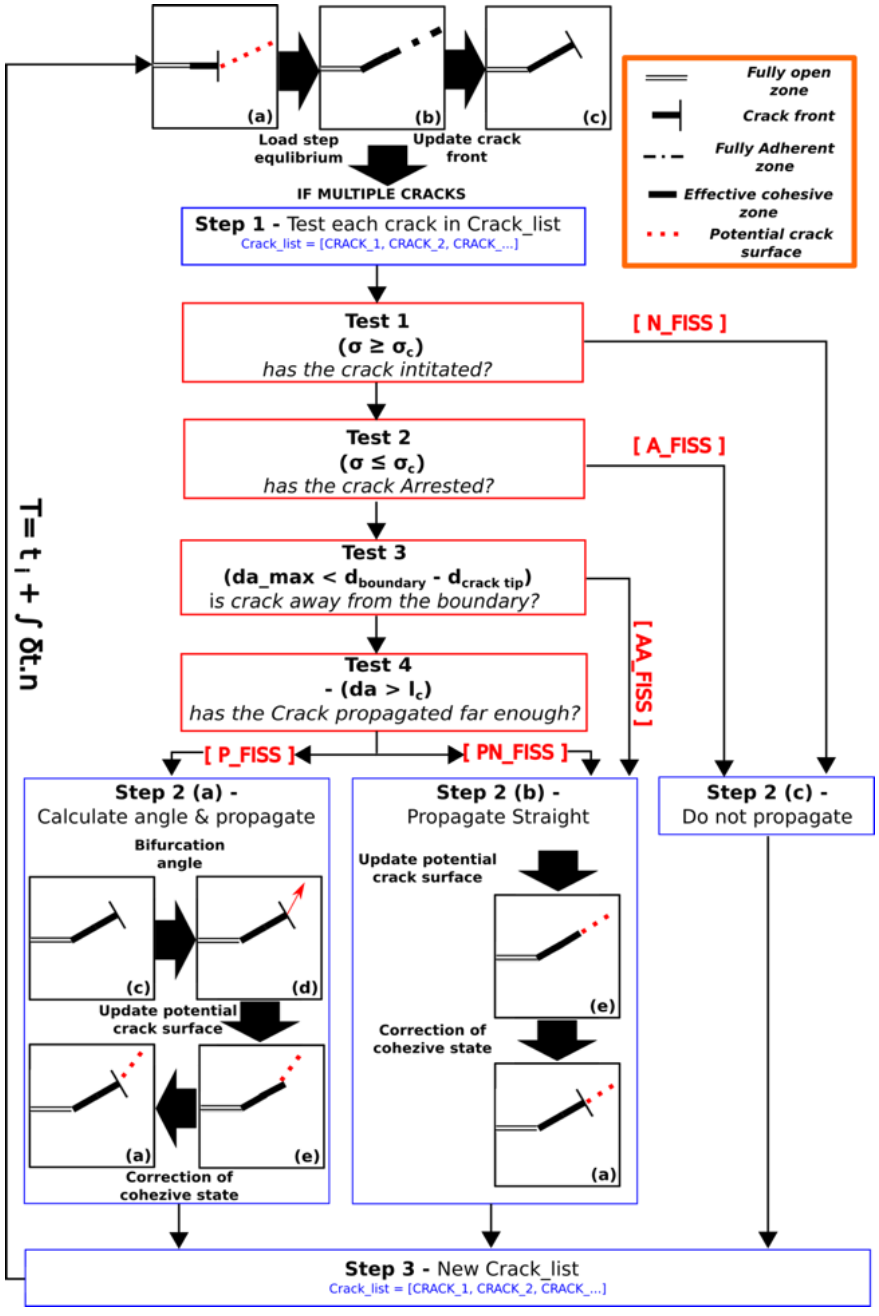

Figure 7. XCZM with multiple cracks algorithm.

MODEL SETUP

The model setup follows on from previous work and applies the macro-fragmentation algorithm to a thin brick slice in Figure 8(a), Crump (2016, 2017). A regular Hexahedral mesh is loaded circumferentially through an applied force h_f, to simulate the stress state experienced post stress reversal. To initiate a crack, a fully adherent cohesive zone is inserted between two elements in the keyway corners as in Figure 8(b). The crack is then initiated by increasing h_f (slowly) until the fracture criterion is attained with the properties used in Table 1.

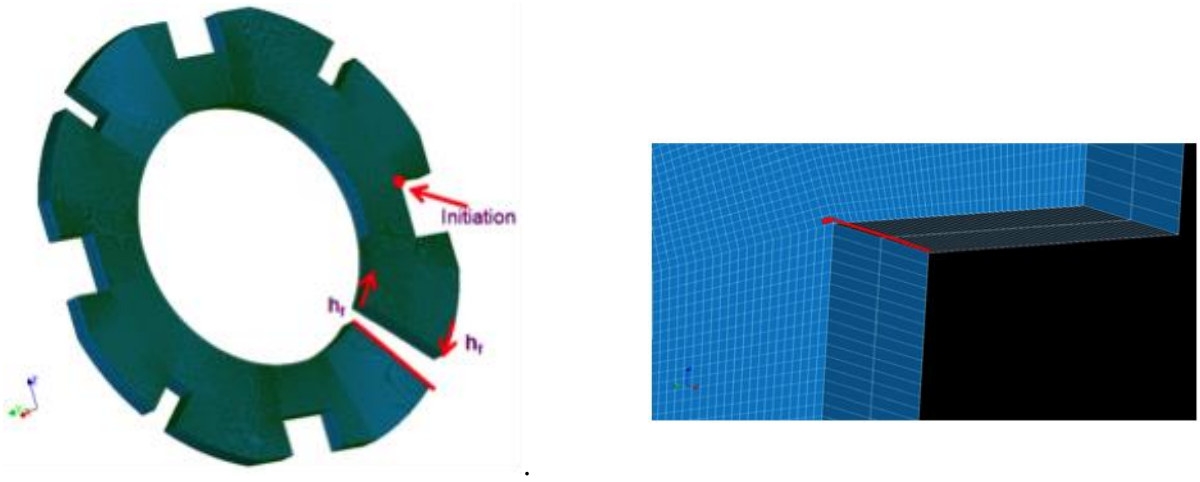

(a) (b)

Figure 8. (a) Thin slice 3D graphite brick mesh and loading used; (b) Inserted initial cohesive zone.

Table 1: Properties used in the model

Parameter	Value
Young's Modulus [GPa]	10
Density ρ [kgm^{-3}]	1800
Poisons ratio	0.2

Parameter	Value
G_c [Jm^{-2}]	140
σ_c [MPa]	25
h_f [kN]	80

PRIMARY CRACK INTERACTION WITH A METHANE HOLE

The first model considers the interaction of an on-the-fly dynamic crack with a methane hole placed 2/3's along the crack path, where the dynamic effects are expected to be the most significant in interaction, Crump (2017). The results of this can be seen in Figure 9. Evidently the methane hole deflects the crack around the hole; the crack would otherwise propagate through the position of the methane hole if it were not present.

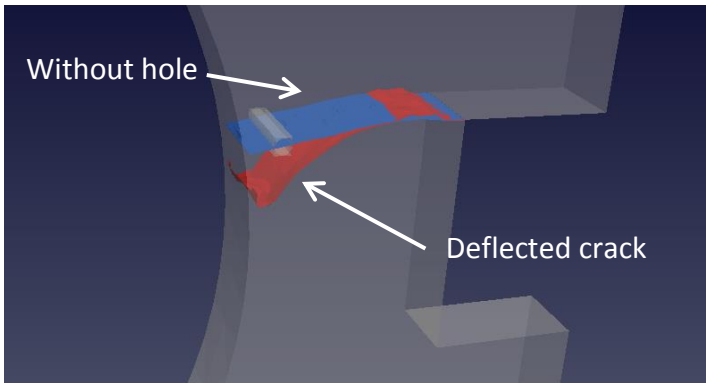

Figure 9. Comparative crack paths due to methane hole interaction.

PRIMARY CRACK PROPAGATION THROUGH AN UNDULATING POTENTIAL

The second model considered the primary crack proapagting through an undulating potential in Figure 10(a). The avalible G_c was abruptly changed by 10% every 1mm to simulate the 'maximal' heterogeneity which maybe observed from graphites micro-texture below l_c. The results of this can be seen in Figure 10(b). Dynamic fracture theory states (Freund (1990)) that crack initiation is goverend by σ_{max} whereas crack propagation is goverened more by the (average) bulk properties of the material. This can be seen through the larger initation angle in Figure 10(b) with minimal difference in the profile later on when using a fixed G_c in Figure 9.

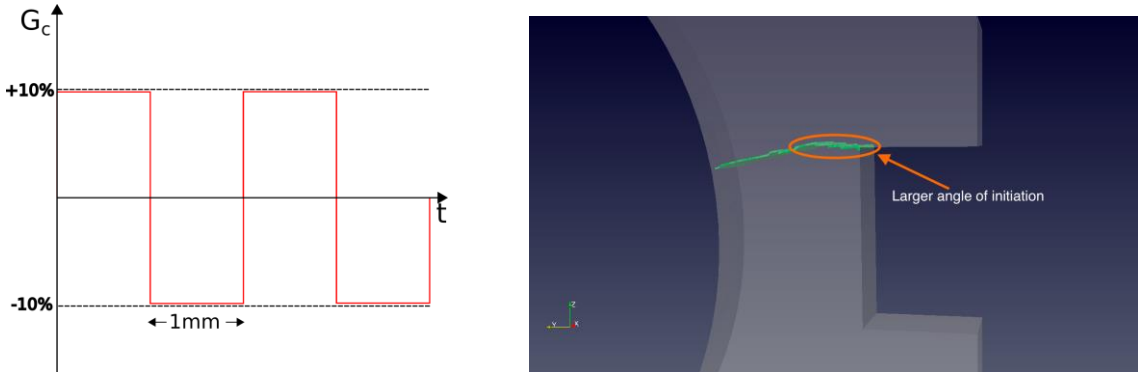

(a) (b)

Figure 10. (a) Periodic profile observed by a propagating crack; (b) Resultant crack profile.

3D ON-THE-FLY PSC

To consider the PSC mechanism, a fully adherent cohesive zone is inserted into keyway corners directly opposite each other (as in Figure 8(b)). The stress profiles for 4 important times in the PSC mechanism can be seen in Figure 11. It is clear that the path of the dynamically initiated crack starts by propagating towards the higher KE region before progressing towards the bore. This can be observed more clearly when the primary and secondary crack profiles are overlaid in Figure 12.

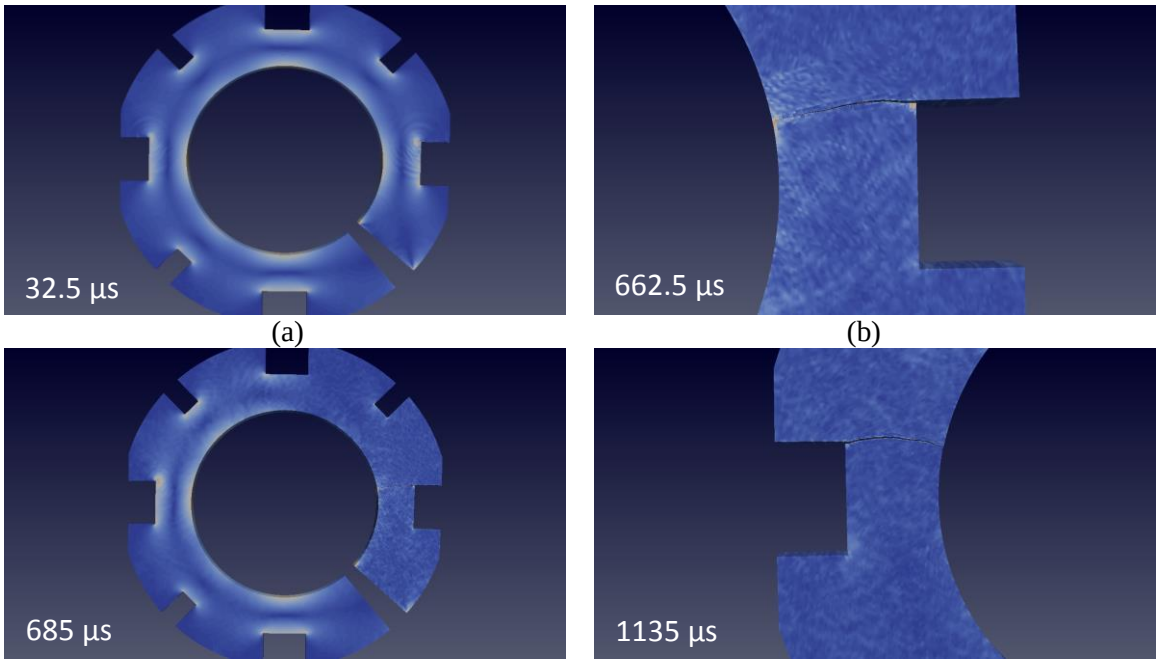

(a) (b) (c) (d)

Figure 11. Important times thought-out the PSC mechanism: (a) Primary crack initiation; (b) Primary crack breaking through bore; (c) Secondary crack initiation; (d) Secondary crack breaking through bore.

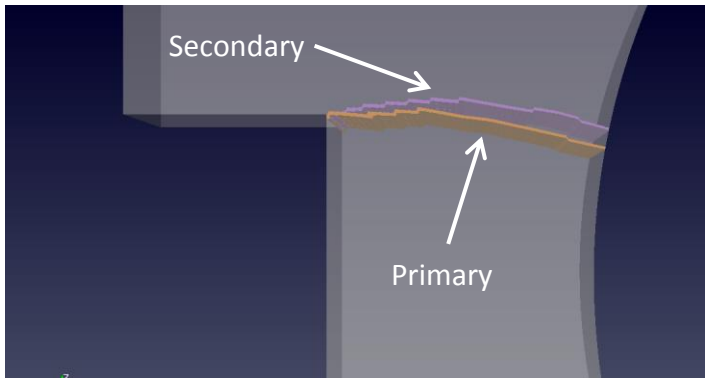

Figure 12. Overlay of the Primary and Secondary crack paths.

CONCLUSION

This paper considered dynamic fracture of graphite and the PSC mechanism in graphite brick slices using a multiple crack algorithm developed for use with the XCZM crack propagation approach. There were 3 main models considered: on-the-fly crack interaction with a methane hole, dynamic cracks propagating through an undulating potential and finally an on-the-fly secondary crack profile. The following conclusions can be made:

- The presence of methane holes can lead to crack path deflection into an ‘s-shape’ profile with associated increase of energy dissipated in fracture;
- Graphite heterogeneity, represented by undulating fracture energy of 10%, does not significantly affect the crack profile;
- Prompt Secondary Cracking may occur with the crack path governed by kinetic energy, i.e. propagation towards the higher KE region is observed.

AKNOWLEDGEMENTS

The main author would like to thank: the on-going support of EPSRC through the Engineering Doctorate Training Centre (EP/G037426/1), the Dalton Nuclear Institute and the insight given by his previous and current supervisors at the University of Manchester in producing this work.
The authors gratefully acknowledge EDF Energy Generation for their valuable input data and support. The views expressed in this paper are those of the authors, and not necessarily those of EDF Energy Generation. Technical support for this work from EDF R&D is greatly appreciated.

REFERENCES

BBC (2014). New cracks in Hunterston reactor. URL https://goo.gl/v4DgrR
BBC News (2016). Inside out west, 2016. URL https://goo.gl/7z6So4
Crump T, Ferte G, Jivkov AP, Mummery P. 3D Dynamic Crack Propagation within AGR Graphite Bricks 3D Dynamic Crack Propagation within AGR Graphite Bricks. *5th EdF Energy Nucl Graph Conf.* 2016;(May).
Crump T, Mummery P, Jivkov A, Tran V-X. A meso-scale approach to modelling stable dynamic crack propagation in glass under rate-dependent loading. *Procedia Struct Integr* [Internet]. Elsevier B.V.; 2016;2:381–8. Available from: http://linkinghub.elsevier.com/retrieve/pii/S245232161630049X
Crump T, Ferté G, Jivkov A, Mummery P, Tran V-X. Dynamic fracture analysis by explicit solid dynamics and implicit crack propagation. *Int J Solids Struct* [Internet]. Elsevier Ltd; 2017 Apr;110–111:113–26. Available from: http://linkinghub.elsevier.com/retrieve/pii/S0020768317300343
Crump T, Ferté G, Mummery P, Jivkov A, Martinuzzi P, Tran V-X. Dynamic fracture effects on remote stress amplification in AGR graphite bricks. *Nucl Eng Des* [Internet]. 2017 Jan;1–10. Available from: http://linkinghub.elsevier.com/retrieve/pii/S0029549317300146
DECC (2015). Updated energy and emissions projections 2015. URL https://goo.gl/Rt5GeW
Doyen D, Ern a., Piperno S. Quasi-explicit time-integration schemes for dynamic fracture with set-valued cohesive zone models. *Comput Mech*. 2013;52(2):401–16.
Ferté .G. Mansouri.A. (2014). "Propagation De Fissures Cohesives En 3 Dimensions". EDF R&D, Fr.
Freund L. B. (1990). "Dynamic Fracture Mechanics". Cambridge Univ Press Cambridge Massachusetts.
IAEA (2016). Graphite in the Advanced Gas Reactor Fleet, 2016. URL http://goo.gl/gfDWk5 .
Kanninen. M.F. and C.L. Popelar. (1985). "Advanced fracture mechanics". Oxford University Press.
Kuroda, M., Fok, S. L., Marsden, B. J., Oyadiji, S, O. (2005) "Dynamics and generation of stress waves in cracked graphite moderator bricks". Nuclear Engineering Design ;235(5):557–73.
Marsden BJ, Haverty M, Bodel W, Hall GN, Jones AN, Mummery PM, et al. Dimensional change, irradiation creep and thermal/mechanical property changes in nuclear graphite. *Int Mater Rev* . Taylor & Francis; 2016 Apr 2;61(3):155–82.
Meyers .A.(1994). "Dynamic Behaviour Of Materials". *John Wiley & Sons.*
Moës N, Dolbow J, Belytschko T. (1999) A finite element method for crack growth without remeshing. *Int J Numer Methods Eng*. John Wiley & Sons, Ltd.; Sep 10;46(1):131–50.
Neighbour (2007) G B Neighbour. Management of Ageing Processes in Graphite Reactor Cores, volume 309. *Royal Society of Chemistry*, 2007
ONR (2015). EDF Energy Nuclear Generation Ltd (NGL) Heysham 1 / Hartlepool and Heysham 2 / Torness Plant Life Extension (PLEX):Project Assessment Report, ONR-CNRP-PAR-15-005. URL https://goo.gl/KxP4gm
Ravi-Chandar. K. and Knauss. W.G. (1984). "An experimental investigation into dynamic fracture. part ii : microstructural aspects". *International Journal of Fracture*, 26:141-154.
Zhou, J.F., Molinari, and Shioya, T. (2005) "A rate-dependent cohesive model for simulating dynamic crack propagation in brittle materials". *Engineering fracture mechanics*, 72:1383 -1410, 2005.